

# A numerical investigation of chamber size and boundary effects on the helix bearing resistance of helical piles in sand

Diego Moreira da Silva  
EESC/USP, São Carlos, Brazil, eng.laum@gmail.com

Cristina de Hollanda Cavalcanti Tsuha  
EESC/USP, São Carlos, Brazil, chctsuh@sc.usp.br

**ABSTRACT:** Currently, a large calibration chamber is being constructed at the University of São Paulo to investigate the behavior of helical foundations installed in instrumented soil samples. For the design of this chamber, a numerical study was carried out using Plaxis 2D software to evaluate the effect of the chamber size and boundary conditions on the helix bearing resistance under tension and compression static loadings. Additionally, in this work the influence of the size of the central hole of the annular pressurized membrane (central space for the pile shaft installation) on the stresses in the soil sample was evaluated numerically. To evaluate the influence of the size of the calibration chamber on the pile response, tensile and compressive loadings on a helical pile model were numerically simulated, considering the installation effect on the soil above the helix. The results indicate that for a calibration chamber of 1.20 m diameter and 1.50 m height, the use of a pressurized membrane with a central hole of 100 mm diameter does not influence the model pile response. Also, the investigated chamber size is suitable to study the response of helical foundations using a model of a pile section with helices in sizes up to 200 mm diameter.

**KEYWORDS:** Calibration chamber, helical foundations, numerical analysis.

## 1 INTRODUCTION

Helical piles are composed of one or more helical-shaped circular plates welded to a central steel shaft. During installation, they are "screwed" into the ground by the application of a torque to the top of the rod, with a penetration rate of one pitch per revolution. This type of foundation has been widely used to resist tensile and compressive forces in transmission line towers, solar panels, wind towers and other types of structures.

The current understanding of the behavior of this type of pile is still limited, and the existing methods to estimate the ultimate uplift or compressive capacity are not satisfactory. One of the reasons for this observed discrepancy between predicted and measured load capacities is the effect of the installation not being considered in the predictions. During the

installation process, the helical pile penetrates into the ground causing torsional and vertical shearing, the soil is displaced laterally and the surrounding soil stresses are modified. The cylinder of soil penetrated by the helical pile is disturbed and this disturbance influences the uplift response of the pile.

Under the scenario described above, experimental investigations are necessary for a better understanding of the behavior of helical foundations. In field tests, the soil conditions are normally not controlled. However, for the tests carried out on physical models in the natural scale or with reduced size, most of the environmental soil conditions can be reproduced. The calibration chambers tests is a physical model technique that allow the use of soil samples under known and controlled stresses.

An example of the use of a calibration

chamber to investigate the behavior of pile foundations is presented in Figure 1. Foray et al. (1998) used calibration chamber tests to investigate the effect of overconsolidation on the bearing capacity of piles driven into dense sands. For this study, the sand sample preparation was interrupted for placing total stress at different depths in the chamber. These cells were used to follow the variations in the sand mass during installation of the pile and during static pile load testing.

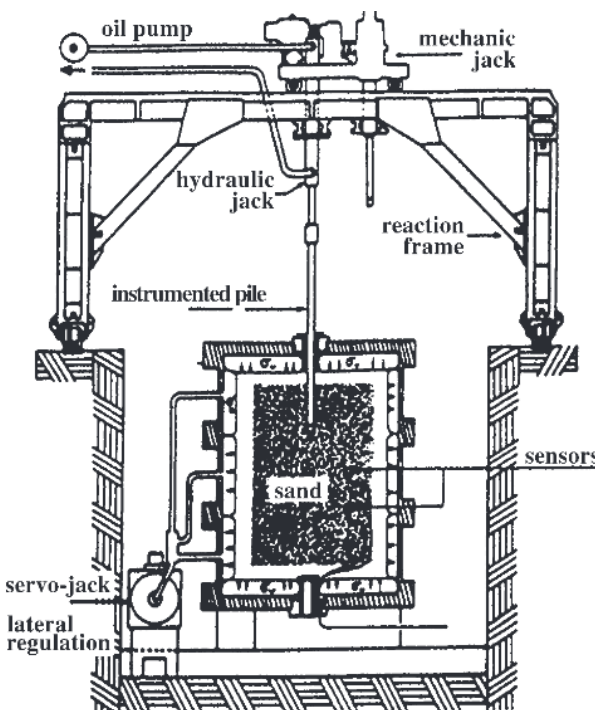


Figure 1. Schematic of the INPG calibration chamber (Foray et al., 1998)

In order to investigate the helical pile response under tensile and compressive loadings, a large calibration chamber is being constructed at the University of São Paulo. For the design of this chamber, numerical simulations were carried out to evaluate if the size of the calibration chamber was large enough to prevent boundary effects. These numerical simulation was performed using the finite element program PLAXIS 8.5.

The soil used for the simulation is the fine sand tested in the centrifuge models of Schiavon (2016). The numerical analysis was divided into two phases: (1) evaluation of the

influence of the diameter of the central hole of the membrane used to apply pressure to the sand sample; (2) verification of the influence of the size of the calibration chamber on the response of tensile and compressive loading tests on a helical pile model.

## 2 NUMERICAL MODELING

### 2.1 Soil parameters

The sand sample used in the numerical simulations for the installation of the pile model is the sand used and described in Schiavon (2016). The soil is a dry fine-grained Hostun sand (HN38), with relative density ( $D_r$ ) of 99%. Table 1 shows the main characteristics of the sand.

Table 1. Sand parameters of the Hostun sand (Schiavon et al. 2017).

Specific gravity of the sand particles	$G_s$	2.64*
Maximum dry density: kg/m <sup>3</sup>	$\rho_{d(max)}$	1554
Minimum dry density: kg/m <sup>3</sup>	$\rho_{d(min)}$	1186
Sand sample average dry density: kg/m <sup>3</sup>	$\rho_d$	1551
Average grain size: mm	$d_{50}$	0.12
Coefficient of uniformity	$C_u$	1.97
Relative density: %	$D_r$	99†
Friction angle from direct shear tests: deg	$\phi_{ds}$	48
Friction angle from triaxial tests: deg	$\phi_{tr}$	47

\*Tests results performed by Unisol Laboratories.

†Estimated from at least two calibrated boxes placed on the bottom of the strongbox.

### 2.2 Calibration of the soil parameters by numerical simulation of triaxial tests

For the calibration of the soil parameters used in the numerical model, triaxial compression tests were simulated in PLAXIS version 8.5. By comparing the best fit between the numerical results and the experimental curves of triaxial tests presented in Schiavon (2016), it was possible to obtain the soil parameters to be used as input data of the numerical modeling. For this comparison, an axisymmetric model (1.0 m x 1.0 m) was used (Figure 2).

The dimensions shown in figure 2 are not realistic, but they are chosen for simplicity (the size of the soil model does not influence the

results). In this configuration the stresses and strains are uniformly distributed over the geometry. The constitutive model used in this simulation was the Hardening-Soil (HS).

Figure 3 shows the best fit obtained between the simulation results and the experimental results of the triaxial tests for confining stresses ( $\sigma_3$ ) of 50, 100 and 200KPa.

From the numerical adjustment shown in figure 3, the obtained strength and stiffness parameters are presented in Table 2. These parameters were used in the numerical model to simulate the behavior of the undisturbed sand during loading tests on the helical pile.

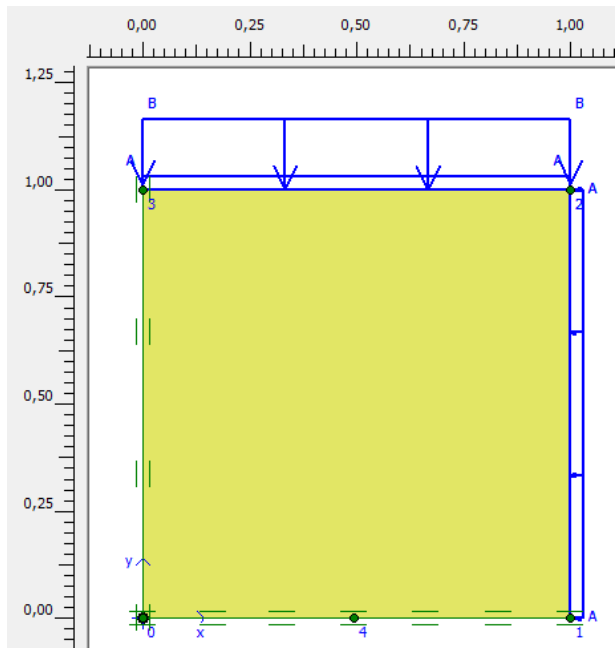


Figure 2. Geometry of the sand specimen in PLAXIS 8.5.

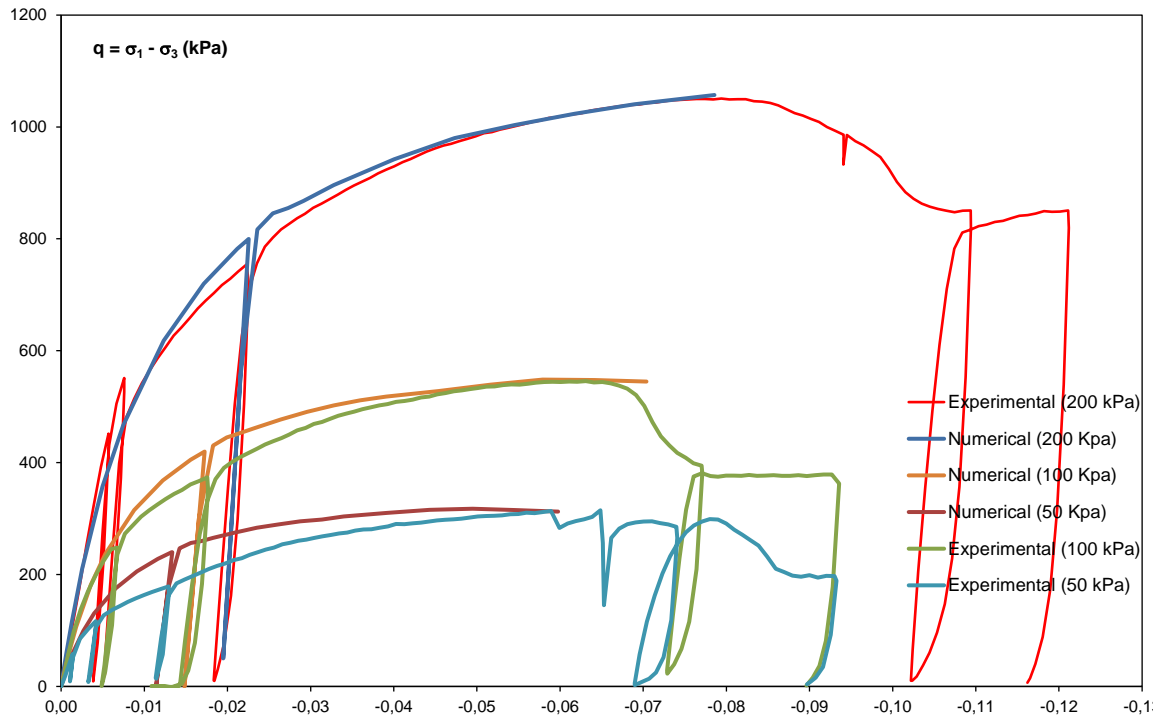


Figure 3 - Comparison between the numerical and experimental results of the triaxial tests of Schiavon (2016) for (a)  $\sigma_3 = 50$  KPa, (b)  $\sigma_3 = 100$  KPa; and (c)  $\sigma_3 = 200$  KPa.

### 2.3 Geometry of the numerical model

The numerical simulations were performed using a two-dimensional axisymmetric model with the vertical axis of symmetry passing through the center of the pile, as shown in

figure 4. The axisymmetric model is used for circular structures with a uniform radial cross section and loading scheme around the central axis, where the deformation and stress state are assumed to be identical in any radial direction.

The generation of the mesh was done

through the option "generate mesh". For a first analysis, the "coarse" option was used for all the geometries (soil, shaft, helical plates, etc.). The top part of the model is a free surface located at  $y = 1.50$  meters from the bottom.

The mesh representing the soil mass was divided into 2 clusters based on the geometry shown in figure 4. Cluster 1 is the natural soil not disturbed by the installation of the helical pile. Cluster 2 is the disturbed soil above the plate that was "loosened" during the helical pile installation. Finally, Cluster 3 represents the steel helical pile.

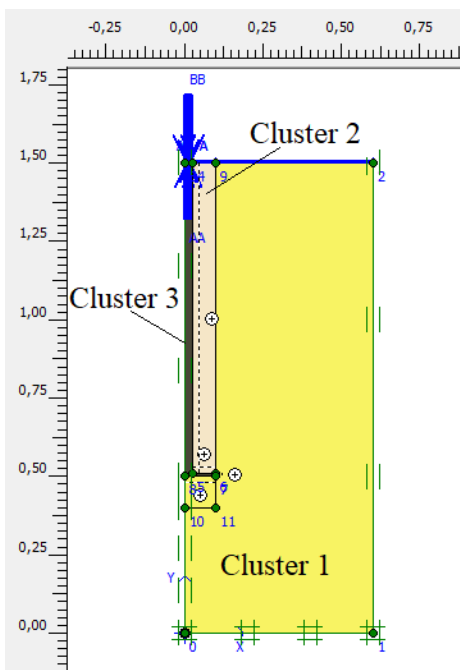


Figure 4 - Geometry of the numerical model in PLAXIS

#### 2.4 Material properties and constitutive models

The numerical models performed involves 2 main materials: steel of the helical pile and the sand (undisturbed and disturbed). For the steel, the linear elastic model was used. The properties considered in the numerical model are: Stiffness modulus ( $E = 200$  GPa), Poisson's ratio ( $\nu = 0,15$ ), and Unit weight ( $\gamma = 70$  KN/m<sup>3</sup>).

The sand was simulated using the constitutive model Hardening soil, which is based on the Mohr-Coulomb (MC) model. For

the Hardening-Soil (HS) model (similarly to the Mohr-Coulomb model) the stress limit state is described by the friction angle ( $\phi$ ), cohesion ( $c$ ) and dilation angle ( $\psi$ ). The mechanical properties of the intact soil were obtained based on the calibration of the triaxial tests presented in Figure 2. Table 2 shows the parameters considered in the numerical simulation of the undisturbed and disturbed sand.

The mechanical properties of the disturbed soil (cylinder of soil disturbed by the installation of the helical pile) were established by the reduction of soil resistance and stiffness parameters. Pérez (2017) performed several parametric analyzes varying the sand friction angle and the Young modulus of the disturbed sand of Schiavon (2016) until reaching a good agreement between experimental and numerical results of load-displacement curves obtained from tensile load tests on a single-helix anchor in centrifuge. In this cited work, the elastic modulus found for the disturbed soil was 80% of the value of the intact soil. For the current numerical study, to simulate the disturbed soil the same reduction in the elastic modulus was adopted, and a friction angle of 37° was used.

Table 2. Properties of the undisturbed (Cluster 1) and disturbed sand (Cluster 2).

Properties	Unit	Symbol	natural sand	disturbed sand
elastic modulus	MPa	$E$	40	32
Poisson's ratio	-	$\nu$	0.3	0.3
Friction angle	°	$\phi$	47	37
Dilatancy angle	°	$\psi$	16	0
Cohesion	KPa	$c$	0	0

#### 2.5 Numerical analysis

The numerical analysis performed is divided into three steps: (1) initiation of stresses with the installed helical pile, (2) tensile loading; and (3) compressive loading.

In the first step, four different conditions of initial soil stresses after the installation of the pile were simulated: (1) no pressure applied to

the membrane on top of the sand sample; (2) applied pressure of 50 KPa on the top of the sand sample; (3) applied pressure of 100 KPa on the top of the sand sample; and (4) applied pressure of 150 KPa on the top of the sand sample.

In the second step, a tensile loading was applied to the pile head to simulate the pile pullout test. For the four different conditions of stresses in the soil (simulation of four different depths of the bottom section of the pile) the tensile force was increased until a maximum value.

In the third step, a compressive loading was applied to the pile head [in Plaxis compression is taken as negative (-)] to simulate the pile under compressive loading. For the four depth conditions evaluated, the compressive loading was increased until a maximum value.

### 3 RESULTS AND DISCUSSION

#### 3.1 Influence of the size of the central hole of the membrane

In order to evaluate the importance of considering the effect of the central hole of the pressurized membrane on the load-displacement response of helical piles, initially a simulation was performed in which the top of the sand sample was submitted to a pressure of 50 kPa and 150 kPa.

The calibration chamber is 1.50 meters high and 1.20 meters in diameter. As it is an axisymmetric model, the geometry to be drawn in PLAXIS 8.5 was 1.5m high and 0.6m in diameter.

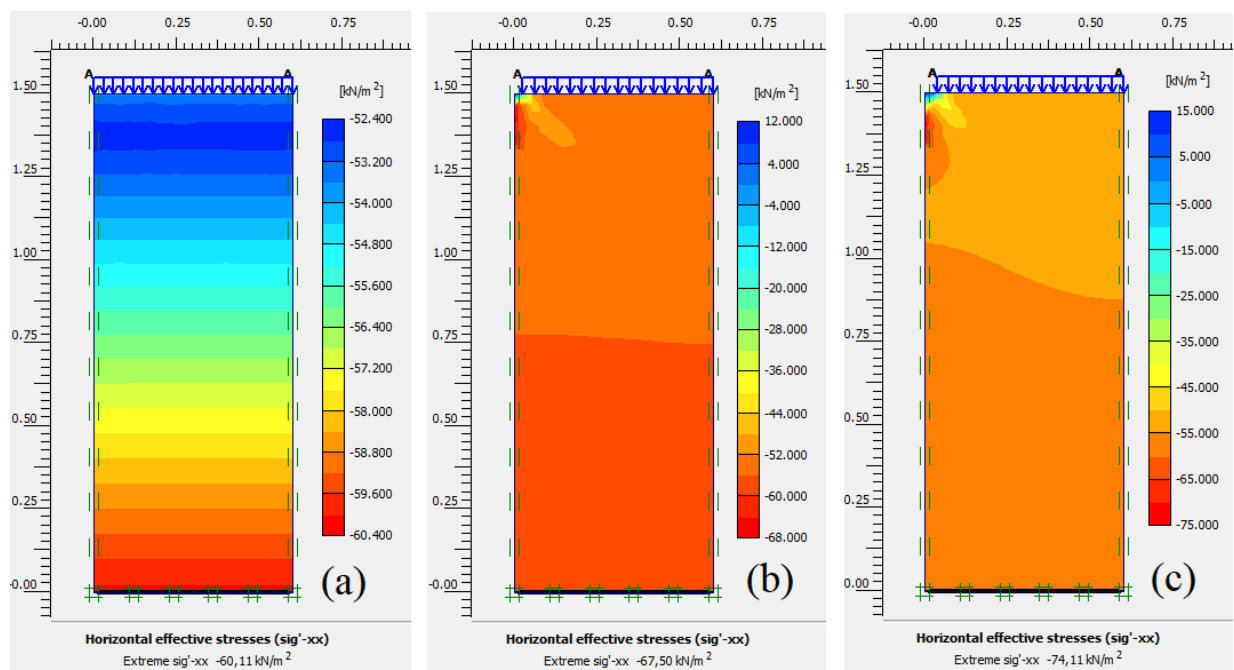


Figure 5 – Vertical stresses for the applied pressure of 50 kPa: (a) without the central hole; (b) hole diameter of 50 mm; (c) hole diameter of 75 mm.

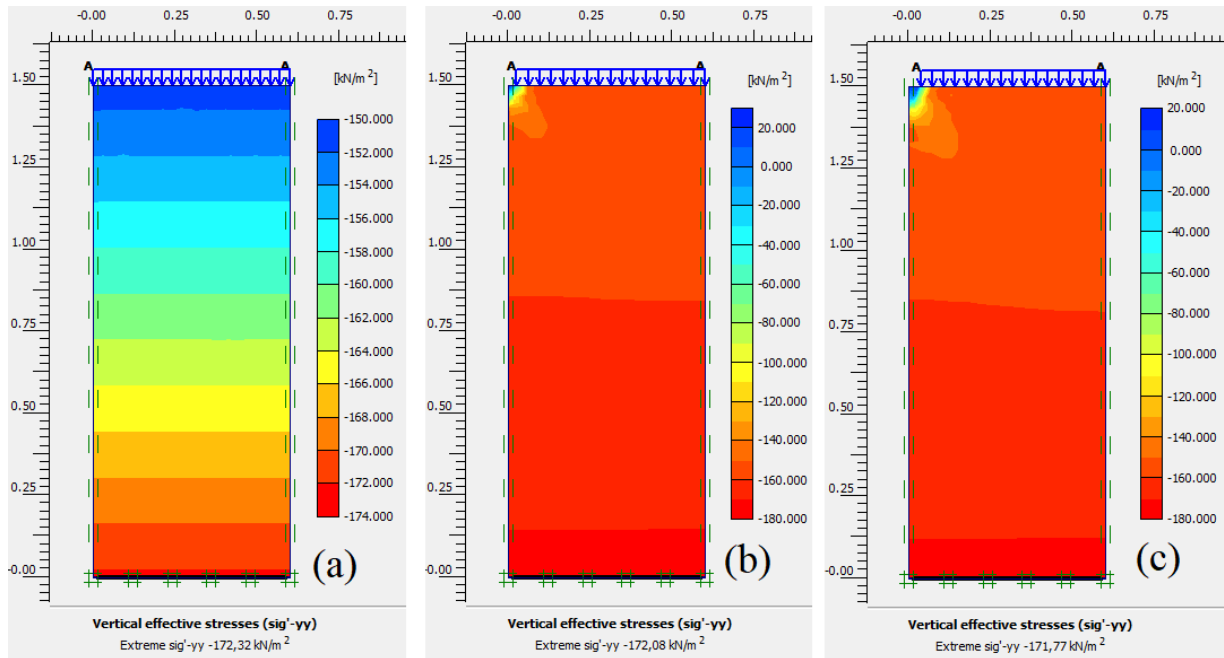


Figure 6 - Vertical stresses for the applied pressure of 150 kPa: (a) without the central hole; (b) hole diameter of 50 mm; (c) hole diameter of 75 mm.

The sand sample under an applied pressure of 150 KPa (Figure 6) simulates the field soil at a depth of approximately 10 meters depth. Figure 5 and 6 illustrates the initial geostatic stresses before the helical pile installation. It can be seen in these figures that the larger the diameter of the central hole the greater the zone influenced by the hole.

These simulations are very important to help the decision about the minimum depth needed to install the helical plate of the model pile (for tensile loading tests) to prevent any effect of the membrane hole.

The influence of the central hole of the membrane on the vertical stresses shown in Figures 5 and 6 indicate that the membrane of 50 mm radius is suitable for the simulation of the sand sample. Therefore, this size of central hole was chosen for the current study.

### 3.2 Influence of the size of the calibration chamber

After the installation of the helical pile, a cylindrical column of soil is disturbed by the

penetration of the helical plate. Since the degree of disturbance is not known, the parameters of the disturbed soil described in table 2 were reduced in relation to the intact soil.

For the evaluation of the influence of the size of the calibration chamber chosen on the results of the loading tests on a single helix-pile, the contours of vertical and horizontal displacements were examined numerically.

Four different values of pressure applied by the upper membrane on the top of the sand sample to simulate different conditions of the depth of the bottom section of a helical pile were evaluated: (1) no pressure; (2) applied pressure of 50 KPa; (3) applied pressure of 100 KPa; and (4) applied pressure of 150 KPa. A helical plate of 200 mm diameter was adopted for the simulations.

Figure 7 and figure 8 show the vertical and horizontal displacements caused by a tensile loading (maximum value) applied on the bottom section of a helical pile, under the four different stresses conditions mentioned above (helical plates installed at different depths).

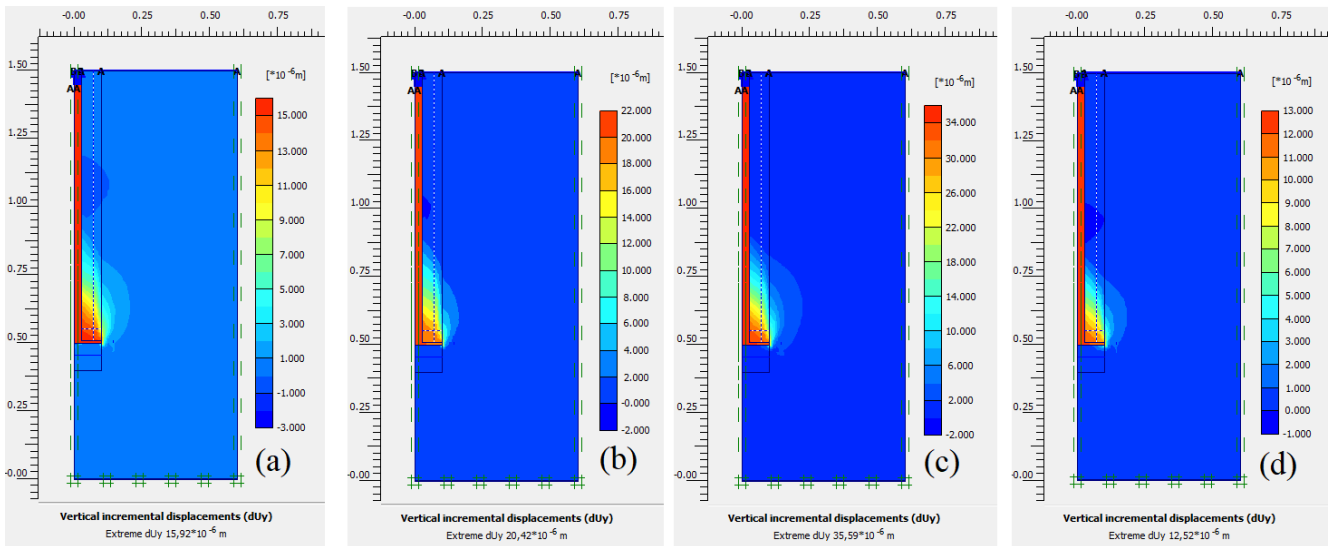


Figure 7 - Vertical displacement contours during the tensile loading (a) no pressure; (b) 50 KPa; (c) 100 KPa; and (d) 150 KPa.

As expected, with increasing the applied pressure at the top of the sand sample (simulating the increase in the depth of the helical plate) the vertical displacements decrease (figure 7). It can be seen that the largest

displacements are concentrated within the disturbed soil cylinder. In all cases the displacements does not reach the edges of the calibration chamber.

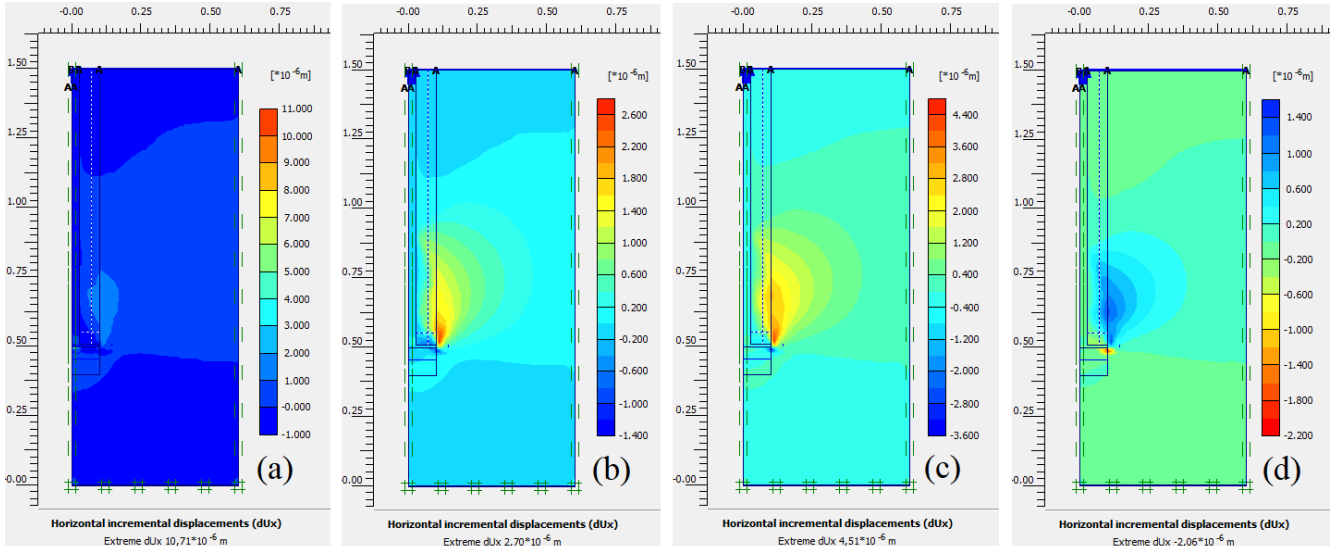


Figure 8 - Horizontal displacement contours during a tensile loading applied to the helical pile: (a) no pressure; (b) 50 KPa; (c) 100 KPa; and (d) 150 KPa.

Figure 8 indicates a concentration of horizontal displacement along the outer perimeter of the helix at the interface between disturbed and undisturbed soil. As the applied pressure to the top of the sand increases, the horizontal displacements increases, especially in the zone just above the helical plate. For the

cases of applied pressure of 100 and 150 KPa the displacements reach the edges of the calibration chamber, however, these displacements are very small ( $0.8 \times 10^{-6}$  mm) and can be considered insignificant.

Figures 9 and 10 show the vertical and horizontal displacements caused by the

compressive loading applied on the bottom section of a helical pile. Figure 9 shows that the largest displacements occur beneath the helical plate, as expected for a compression test. In all cases the displacements do not reach the base of the calibration chamber.

Figure 10 indicates a concentration of horizontal displacements bellow the helical plate. With increasing the pressure on the top of the sand sample the horizontal displacements increase. The largest displacements are concentrated below the helical plate in the zone of undisturbed soil in the form of a “water drop” (Figure 10(a) in yellow and figure 10b, in blue).

In the case of compressive loading, the

vertical and horizontal displacements that reach the edges and the bottom of the calibration chamber are very small, and can be considered insignificant.

Therefore, for this calibration chamber and model pile configurations, in which the distance between the bottom of the chamber and the helical plate is 2.5 times the diameter of the helix (50 mm), and the horizontal distance between the edge of the plate and the chamber wall is also 2.5 times the diameter of the helix, the edge of the chamber seems to not affect the load tests results.

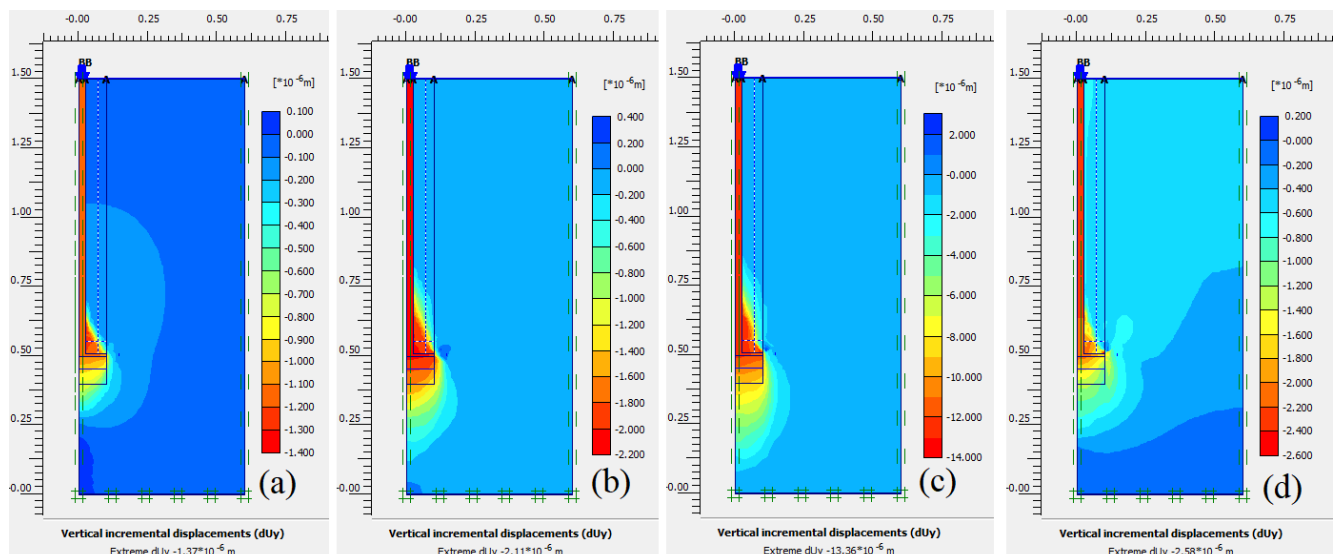


Figure 9 – Vertical displacement contours during compressive loading: (a) no pressure; (b) 50 KPa; (c) 100 KPa; and (d) 150 KPa.

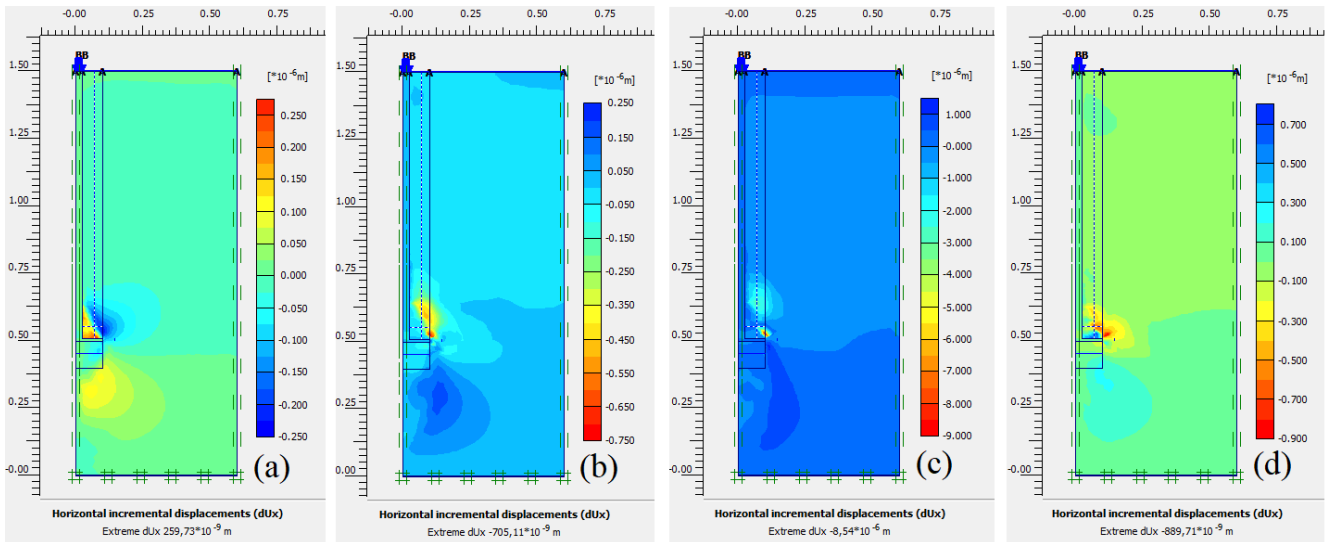


Figure 10 - Horizontal displacement contours during compressive loading: (a) no pressure; (b) 50 KPa; (c) 100 KPa; and (d) 150 KPa.

## 4 CONCLUSIONS

The numerical simulations carried out in this work showed that for the size of calibration chamber investigated: (1) the pressurized membrane with a central hole of 50 mm radius is suitable for tests on helical pile models; (2) for applied pressures on the top of the sand sample of 50 KPa, 100 KPa and 150 KPa there is no influence of the calibration chamber size for a pile with a 200 mm helical plate. Therefore, the calibration chamber of 1.20 m diameter and 1.50 m height are adequate for carrying out the loading tests on helical pile models with helices in sizes up to 200 mm diameter.

## ACKOWLEGEMENTS

The authors would like to thank José Schiavon for the sand data used for the simulations, and to Professor Daniel Dias for assisting in numerical modeling.

## REFERENCES

Foray, P., Balachowski, L., & Colliat, J. L. (1998). Bearing capacity of model piles driven into dense

overconsolidated sands. *Canadian Geotechnical Journal*, 35(2), 374-385.

Pérez, Z. A. (2017) *Numerical analysis of the effect of installation of helical anchors in sand*. MSc thesis – School of Engineering of São Carlos, University of São Paulo, São Carlos, 157p.

Plaxis, B. V. *PLAXIS 2D Version 8.2-Finite element code for soil and rock analysis*. AA Balkema, Delft (2004).

Schiavon, J. A. (2016) *Behaviour of helical anchors subjected to cyclic loadings*. Ph.D. Thesis, São Carlos school of Engineering, University of São Paulo, São Carlos, 300p.

Schiavon, J. A., Tsuha, C. H. C., & Thorel, L. (2017). Cyclic and post-cyclic monotonic response of a single-helix anchor in sand. *Géotechnique Letters*, 7(1), 11-17.